10c is most plausible for (12,7,1). This structure is closely related to the structure of $(C_6H_5As)_2Mo_6O_{25}H_2^{4-}$.[17] It has a tetrahedral Mo group instead of the second heteroatom group. The species (11,7,1) is then easily explained by the dissociation of one of the protons of the water molecule, which is indicated by an open circle in Figure 10c. If we remove the $MoO_4^{2-}$ group from this structure and rearrange the atoms, it turns out to be the structure of (12,6,1), which is shown in Figure 10d. The $CH_3AsMo_6O_{21}(H_2O)_6^{2-}$ anion has been reported to have a similar structure.[18] The structures in Figure 10c,d are thus proposed as the solution structures for (12,7,1) and (12,6,1). Considering the fast exchange between the two species, even from an NMR point of view this pair seems credible.

### Concluding Remarks

The results obtained in the system are summarized in Table XII. Although the speciation may seem rather simple, the establishing of the equilibrium model was very tedious and not at all straightforward. As mentioned before, an ordinary $(p,q,r)$ search did not work well for the current system. Figure 5b explains the reason. The observed titration curves at $B/C$ ratios 6 and 15 were quite similar, especially in the range $3.5 > -\lg h > 2$. Moreover, the $Z_{B,C}$ $(=(H-h)/(B+C))$ values in that range were very close to those of the binary molybdate system in the same range. This means that it is difficult to find whether an additional ternary species is formed in this region from emf data alone. Although potentiometry is a powerful tool for investigating solution equilibria, it thus gives an ambiguous result if two or more different species that consume about the same amounts of protons or other ions measured by the electrode are present in solution. This is often the case with polyoxometalates.

On the other hand, the NMR data alone could not lead us to the final model either. It is the combined emf–NMR technique that once again proved to be very powerful for establishing the equilibrium conditions in polyanion systems. It is thereby of vital importance that the NMR data are collected in a quantitative way.

This is the first time we have systematically tested emf and NMR data individually and then the combination. We have therefore chosen to report calculations from different $B/C$ and $-\lg h$ ranges to illustrate all the relevant calculations performed for establishing the final model.

The LAKE program, capable of treating all kinds of information from the combined data, has proved to be very valuable. Although more work has to be done toward a proper way of weighting different kinds of data and different points, the method described in the current paper could be applied to numerous other systems successfully also.

**Acknowledgment.** We thank Professor Nils Ingri and Professor Yukiyoshi Sasaki for their great interest and valuable advice, the members of the NMR group at the Department of Organic Chemistry, Umeå University, for being in charge of the Bruker NMR apparatus, Christina Broman for typing the manuscript, and Lage Bodén for drawing the figures. This work forms part of a program financially supported by the Swedish Natural Science Research Council.

**Registry No.** $MoO_4^{2-}$, 14259-85-9; $C_6H_5PO_3^{2-}$, 16486-11-6.

(17) Matsumoto, K. Y. *Bull. Chem. Soc. Jpn.* **1978**, *51*, 492.
(18) A similar heteropolyanion has been found in the molybdate–methylarsonate system. See: Matsumoto, K. Y. *Bull. Chem. Soc. Jpn.* **1979**, *52*, 492.

Contribution from the Laboratorium für anorganische Chemie, ETH-Z, CH-8092 Zürich, Switzerland, and Istituto di Chimica Farmaceutica, Università di Milano, I-20131 Milano, Italy

# Silver- and Gold-Containing Heterobinuclear Hydrido-Bridged Complexes

Alberto Albinati,[1a] Hans Lehner,[1b] Luigi M. Venanzi,*[1b] and Martin Wolfer[1b]

*Received June 5, 1987*

The hydrido-bridged complex cations $[(PR_3)_2(R')Pt(\mu\text{-}H)M(PR''_3)]^+$ (M = Ag: R = Et, R′ = $C_6Cl_5$, R″ = Et, *i*-Pr, Cy, and Ph; R = Me, R′ = $C_6Cl_5$, R″ = *i*-Pr and Cy. M = Au: R = Et, R′ = $C_6Cl_5$, R″ = *i*-Pr and Ph; R = Et, R′ = $C_6F_5$, and R″ = Ph; R = Et, R′ = Ph, R″ = Ph; R = *i*-Pr, R′ = Ph, R″ = Ph) were prepared from the corresponding *trans*-$[PtH(R')(PR_3)_2]$ and $[M(solv)(PR''_3)]^+$ (solv = THF, $Et_2O$) complexes. Their $^1H$ and $^{31}P$ NMR data are reported together with $^{31}P$ data for the complexes $[Ag(PR''_3)_2]^+$. The X-ray crystal structure of $[(PEt_3)_2(C_6F_5)Pt(\mu\text{-}H)Au(PPh_3)](CF_3SO_3)$ was determined. Its structure is monoclinic, space group $P2_1/c$, with $Z = 4$, $a = 23.609$ (5) Å, $b = 9.725$ (4) Å, $c = 19.683$ (5) Å, and $\beta = 72.91$ (2)°. The final agreement factor (for the 3862 observed reflections) $R$ is 0.043. The structure consists of *trans*-$[PtH(C_6F_5)(PEt_3)_2]$ and "$Au(PPh_3)^{+}$" units held together by the hydride ligand and a Pt–Au bond.

### Introduction

Although several homometallic copper(I) hydrides are known,[2] the corresponding compounds of silver and gold do not appear to have been reported in the literature. However, Wiberg and Henle[3] describe the isolation of $Ag[BH_4]$ and $Ag[AlH_4]$, which decompose at temperatures above −30 and −50 °C, respectively. This ease of decomposition is probably associated with the high oxidation potential of silver ($Ag^+ + e^- \rightarrow Ag$, 0.80 V).[4] Attempts to prepare $AuH_3$, $Au[AlH_4]$, and $Au[BH_4]$ gave products that decompose above −120 °C.[5] Furthermore, the reactions of complexes $[AuX(PR_3)_n]$ with $Na[BH_4]$ produce gold clusters that do not contain hydridic ligands.[6]

As shown by several research groups,[7] unstable mononuclear transition metal hydrides, $L_mMH_x$, can often be stabilized by "coordinating them" to a coordinatively unsaturated metal complex, $M'L'_n$, i.e., by forming species of the type $L_mM(\mu\text{-}H)_xM'L'_n$. Thus, Green et al.[8] reported the isolation of complexes of the types $[(CO)_5M(\mu\text{-}H)M'(PR_3)]$ (M = Cr, Mo, W; M′ = Ag, Au; R = Ph, Me), while Lehner et al.[9] described the preparation of cationic species of the types $[(PPh_3)_3H_2Ir(\mu\text{-}H)Au(PR_3)]^+$ (R = Ph, Et) and $[(PEt_3)_2(C_6Cl_5)Pt(\mu\text{-}H)Au(PEt_3)]^+$ as well as the analogous silver compounds.[10] Since then, many silver- or gold-containing

(1) (a) Università di Milano. (b) ETH Zürich.
(2) (a) Churchill, M. R.; Bezman, S. A.; Osborn, J. A.; Wormald, J. *Inorg. Chem.* **1972**, *11*, 1818. (b) Caulton, K. G. *Ann. N.Y. Acad. Sci.* **1983**, *415*, 27. (c) Lemmen, T. J.; Folting, K.; Huffman, J. C.; Caulton, K. G. *J. Am. Chem. Soc.* **1985**, *107*, 7774.
(3) Wiberg, E.; Henle, W. *Z. Naturforsch. B: Anorg. Chem., Org. Chem., Biochem., Biophys., Biol.* **1952**, *7B*, 757.
(4) Latimer, W. M. *Oxidation Potentials*; Prentice-Hall: New York, 1952; p 343.
(5) Wiberg, E.; Neumaier, H. *Inorg. Nucl. Chem. Lett.* **1965**, *1*, 35.
(6) Malatesta, L. *Gold Bull.* **1975**, *8*, 48.
(7) Venanzi, L. M. *Coord. Chem. Rev.* **1982**, *43*, 251 and references quoted therein.
(8) Green, M.; Orpen, A. G.; Salter, I. D.; Stone, F. G. A. *J. Chem. Soc., Chem. Commun.* **1982**, 813.
(9) Lehner, H.; Matt, D.; Pregosin, P. S.; Venanzi, L. M.; Albinati, A. *J. Am. Chem. Soc.* **1982**, *104*, 6825.
(10) Lehner, H. *Dissertation* No. 7239, ETH Zürich, 1983.

0020-1669/87/1326-3933$01.50/0 

hydrides of other types have been described.[11]

This paper reports a study of hydrido-bridged complexes of silver and platinum and of gold and platinum of the type $[(PR_3)_2(R')Pt(\mu\text{-}H)M(PR''_3)]^+$.

## Experimental Section

**Methods and Materials.** The $^1H$, $^{31}P$, and $^{195}Pt$ NMR spectra were recorded either on a Bruker WM 250 or on WH 90 spectrometer using TMS, 85% $H_3PO_4$, or $Na_2[PtCl_6]$, respectively, as external references. A positive sign of the shift denotes a resonance to higher frequency of the reference. Infrared spectra were measured on a Perkin-Elmer 1430 spectrometer using Nujol mulls. Unless otherwise stated, all manipulations were carried out in air.

Solvents ("purum p.a."), $Ag[BF_4]$, and $AgCF_3SO_3$ were purchased from Fluka AG and used without further purification.

**Intermediates and Complexes.** The complexes $[AuCl(PEt_3)]$,[12] $[AuCl(PPh_3)]$,[13] $[AuCl(P\text{-}i\text{-}Pr_3)]$,[14] *trans*-$[PtH(Ph)(PEt_3)_2]$,[15] *trans*-$[PtH(Ph)(P\text{-}i\text{-}Pr_3)_2]$,[15] *trans*-$[PtH(C_6F_5)(PEt_3)_2]$,[16] *trans*-$[PtH(C_6Cl_5)(PEt_3)_2]$,[17] and *trans*-$[PtH(C_6Cl_5)(PMe_3)_2]$[18] were prepared as described in the appropriate references.

**$[(PEt_3)_2(C_6Cl_5)Pt(\mu\text{-}H)Ag(PEt_3)][BF_4]$, 1a[BF$_4$].** A solution of $[Ag(BF_4)(PEt_3)]$ was prepared in situ by adding $PEt_3$ (21 mg, 0.18 mmol) to a solution of $Ag[BF_4]$ (35 mg, 0.18 mmol) in 10 mL of THF. Solid *trans*-$[PtH(C_6Cl_5)(PEt_3)_2]$ (123 mg, 0.18 mmol) was added, and the resulting solution was stirred for 15 min, filtered over Celite, and reduced to a small volume under reduced pressure. A layer of $Et_2O$ was floated over the above solution and the mixture stored for 2 days at −20 °C. This gave the THF monosolvate as colorless crystals in 65% yield. Anal. Calcd for $C_{28}H_{54}AgBCl_5F_4OP_3Pt$: C, 31.52; H, 5.07. Found: C, 31.24; H, 5.03.

**$[(PEt_3)_2(C_6Cl_5)Pt(\mu\text{-}H)Ag(P\text{-}i\text{-}Pr)_3](CF_3SO_3)$, 1b($CF_3SO_3$).** Solid $AgCF_3SO_3$ (33.8 mg, 0.13 mmol) was added to a stirred solution of $P\text{-}i\text{-}Pr_3$ (21 mg, 0.13 mmol) in ca. 5 mL of $Et_2O$. *trans*-$[PtH(C_6Cl_5)(PEt_3)_2]$ (89.8 mg, 0.13 mmol) was then added. The solution was filtered over Celite and evaporated to a volume of ca. 2 mL under reduced pressure, and a layer of pentane was floated over the residual solution. Upon standing for ca. 12 h at −20 °C, the mixture gave a 72% yield of crystalline product in the form of colorless needles that turned to a white powder upon drying; mp 102 °C. Anal. Calcd for $C_{28}H_{52}AgCl_5F_3OP_3PtS$: C, 30.60; H, 4.77; Cl, 16.13. Found: C, 30.94; H, 4.83; Cl, 15.57.

**$[(PEt_3)_2(C_6Cl_5)Pt(\mu\text{-}H)Ag(PCy_3)](CF_3SO_3)$, 1c($CF_3SO_3$).** A suspension of $PCy_3{\cdot}CS_2$ (166.5 mg, 0.47 mmol) in 5 mL of ethanol was refluxed under a nitrogen atmosphere for 15 min to allow the complete distillation of carbon disulfide. The solution was cooled to room temperature, $AgCF_3SO_3$ (120.0 mg, 0.47 mmol) was added, the solvent was evaporated under reduced pressure, and the residue was extracted with 2 mL of dichloromethane. This solution was added to *trans*-$[PtH(C_6Cl_5)(PEt_3)_2]$ (318.3 mg, 0.47 mmol) in 3 mL of diethyl ether. The resulting solution was evaporated under reduced pressure to ca. 1 mL, and 2 mL of diethyl ether was floated on top of it. The mixture was cooled overnight to −20 °C, and the resulting colorless needles (470 mg, 83%) were filtered off; IR (Nujol) 1750 (br) $cm^{-1}$ ($\nu$(Pt-H-Ag)). Anal. Calcd for $C_{37}H_{64}AgCl_5F_3O_3P_3PtS$: C, 36.45; H, 5.29; P, 10.20; Pt, 16.06. Found: C, 36.46; H, 5.45; P, 9.82; Pt, 15.76.

**$[(PEt_3)_2(C_6Cl_5)Pt(\mu\text{-}H)Ag(PPh_3)][BF_4]$, 1d[BF$_4$].** This complex was prepared in 67% yield as its THF solvate, as described for **1a**, with the solvent mixture THF/pentane used for crystallization. Anal. Calcd for $C_{40}H_{54}AgBCl_5F_4OP_3Pt$: C, 36.30; H, 3.92. Found: C, 36.53; H, 4.01.

**$[(PMe_3)_2(C_6Cl_5)Pt(\mu\text{-}H)Ag(P\text{-}i\text{-}Pr_3)](CF_3SO_3)$, 1e($CF_3SO_3$).** This was prepared as described for **1b** with the following differences: (a) THF was used as solvent and pentane as cosolvent; (b) when the mixture was allowed to stand at −80 °C, the product was obtained in 79% yield as a white powder. Anal. Calcd for $C_{22}H_{40}AgCl_5F_3O_3P_3PtS$: C, 26.04; H, 3.97. Found: C, 25.91; H, 3.83.

**$[(PMe_3)_2(C_6Cl_5)Pt(\mu\text{-}H)Ag(PCy_3)](CF_3SO_3)$, 1f($CF_3SO_3$).** A suspension of $PCy_3{\cdot}CS_2$ (21.0 mg, 0.06 mmol) in 3 mL of ethanol was refluxed under a nitrogen atmosphere for 15 min. The resulting solution was evaporated to dryness under high vacuum; $AgCF_3SO_3$ (15.2 mg, 0.06 mmol), *trans*-$[PtH(C_6Cl_5)(PMe_3)_2]$ (35.3 mg, 0.06 mmol), and 3 mL of diethyl ether were then added. The resulting suspension was vigorously stirred for 2 h in the dark, and then the solid product was filtered off; yield 56.6 mg (85%). Anal. Calcd for $C_{31}H_{52}AgCl_5F_3O_3P_3PtS$: C, 32.81; H, 4.62. Found: C, 32.56; H, 4.57. This solid was directly used for an NMR spectroscopic study, which showed that the solution contained **1f** and small amounts of $[Ag(PCy_3)_2]^+$ and $[(PMe_3)_2(C_6Cl_5)Pt(\mu\text{-}H)Ag(\mu\text{-}H)Pt(C_6Cl_5)(PMe_3)_2]^+$ (see Results and Discussion).

**$[(PEt_3)_2(C_6Cl_5)Pt(\mu\text{-}H)Au(PEt_3)][BF_4]$, 2a[BF$_4$].** This compound was prepared analogously to **2c** below and was recrystallized from MeOH; yield 38%. Anal. Calcd for $C_{24}H_{46}AuBCl_5F_4P_3Pt$: C, 26.58; H, 4.25. Found: C, 26.64; H, 4.21.

**$[(PEt_3)_2(C_6Cl_5)Pt(\mu\text{-}H)Au(P\text{-}i\text{-}Pr_3)](CF_3SO_3)$, 2b($CF_3SO_3$).** A mixture of $[AuCl(P\text{-}i\text{-}Pr_3)]$ (50.0 mg, 0.13 mmol) and $AgCF_3SO_3$ (32.7 mg, 0.13 mmol) was stirred for 1 h in 3 mL of diethyl ether. The AgCl precipitate was filtered off over Celite and the solution added to *trans*-$[PtH(C_6Cl_5)(PEt_3)_2]$ (86.8 mg, 0.13 mmol) in 3 mL of diethyl ether that had been precooled to −40 °C. A white precipitate formed. The solvent was decanted and the solid recrystallized from $CH_2Cl_2$ by adding a layer of diethyl ether on top of the solution, giving 104.5 mg (69%) of product as white needles. Anal. Calcd for $C_{28}H_{52}AuCl_5F_3O_3P_3PtS$: C, 28.31; H, 4.41. Found: C, 28.13; H, 4.46.

**$[(PEt_3)_2(C_6Cl_5)Pt(\mu\text{-}H)Au(PPh_3)][BF_4]$, 2c[BF$_4$].** To a solution of $[AuCl(PPh_3)]$ (94.5 mg, 0.19 mmol) in 5 mL of THF was added $Ag[BF_4]$ (37 mg, 0.19 mmol) in 5 mL of THF. The AgCl precipitate was filtered off over Celite and the solution added to *trans*-$[PtH(C_6Cl_5)(PEt_3)_2]$ (130 mg, 0.19 mmol) in 10 mL of THF that had been precooled to −40 °C. The mixture, which turned slightly brown, was stirred for 15 min at −40 °C concentrated under vacuum to about 5 mL, and filtered through Celite. A layer of 15 mL of ether was added on top of the filtrate and the mixture left to stand at −20 °C, producing 100 mg (43%) of product as colorless needles. Anal. Calcd for $C_{36}H_{46}AuBCl_5F_4P_3Pt{\cdot}C_4H_8O$: C, 36.94; H, 4.15. Found: C, 37.16; H, 3.94.

**$[(PEt_3)_2(C_6F_5)Pt(\mu\text{-}H)Au(PPh_3)](CF_3SO_3)$, 2d($CF_3SO_3$).** This compound was prepared analogously to **2c**. It was crystallized in 64% yield from THF by adding a layer of pentane on top of the THF solution. Anal. Calcd for $C_{37}H_{46}AuF_8O_3P_3PtS$: C, 36.78; H, 3.81. Found: C, 37.03; H, 3.88.

**$[(PEt_3)_2(Ph)Pt(\mu\text{-}H)Au(PPh_3)][BF_4]$, 2e[BF$_4$].** *trans*-$[PtCl(Ph)(PEt_3)_2]$ (700 mg, 1.29 mmol) was added to a solution of $Ag[BF_4]$ (250 mg, 1.29 mmol) in THF. The AgCl precipitate was filtered off, the solution cooled to −40 °C, and $Na[BH_4]$ (90 mg, 2.4 mmol) added. The mixture was stirred for 15 min, 20 mL of methanol added, and then the mixture taken to dryness under reduced pressure. The residue was extracted with benzene and the solution taken to dryness under reduced pressure. The residue was dissolved in methanol, and a solution of $[Au(THF)_x(PPh_3)][BF_4]$ in THF was added (this solution was prepared by reacting $[AuCl(PPh_3)]$ (642 mg, 1.29 mmol) in THF with the stoichiometric amount of $Ag[BF_4]$ and filtering off the AgCl precipitate). The reaction mixture was reduced to 5 mL and filtered over Celite, and a layer of 40 mL of pentane was floated on top of the filtrate. After standing at −20 °C for 1 day, the mixture gave grayish crystals that contained small amounts of product as shown by NMR spectroscopy.

**$[(P\text{-}i\text{-}Pr_3)_2(Ph)Pt(\mu\text{-}H)Au(PPh_3)][BF_4]$, 2f[BF$_4$].** This compound was prepared analogously to **2c**. It was crystallized in 23% yield from THF by adding a layer of diethyl ether on top of the THF solution. Anal. Calcd for $C_{42}H_{63}AuBF_4P_3Pt$: C, 44.25; H, 5.53. Found: C, 44.65; H, 5.61.

**Determination and Refinement of the Structure of $[(PEt_3)_2(C_6F_5)Pt(\mu\text{-}H)Au(PPh_3)](CF_3SO_3)$, 2d($CF_3SO_3$). X-ray Measurements.** Crystals of **2d**($CF_3SO_3$) were obtained as described above. A prismatic crystal was mounted at a random orientation on a glass fiber. Space group and

(11) (a) Hutton, A. T.; Pringle, P. G.; Shaw, B. L. *Organometallics* **1983**, *2*, 1889. (b) Freeman, M. J.; Green, M.; Orpen, A. G.; Salter, I. D.; Stone, F. G. A. *J. Chem. Soc., Chem. Commun.* **1983**, 1332. (c) Howard, J. A. K.; Salter, I. D.; Stone, F. G. A. *Polyhedron* **1984**, *3*, 567. (d) Salter, I. D.; Stone, F. G. A. *J. Organomet. Chem.* **1984**, *260*, C71. (e) Connelly, N. G.; Howard, J. A. K.; Spencer, J. L.; Woodley, P. K. J. *J. Chem. Soc., Dalton Trans.* **1984**, 2003. (f) Rhodes, L. F.; Huffmann, J. C.; Caulton, K. G. *J. Am. Chem. Soc.* **1984**, *106*, 6874. (g) Bachechi, F.; Ott, J.; Venanzi, L. M. *J. Am. Chem. Soc.* **1985**, *107*, 1760. (h) Salter, I. D. *J. Organomet. Chem.* **1985**, *295*, C17. (i) Ott, J. Dissertation No 8000, ETH Zürich, 1986. (j) Brown, S. S. D.; Colquhoun, I. J.; McFarlane, W.; Murray, M.; Salter, I. D.; Sik, V. *J. Chem. Soc., Chem. Commun.* **1986**, *53*, 600. (k) Braunstein, P.; Gome, S.; Carneiro, T. M.; Matt, D.; Tiripicchio, A.; Tiripicchio Camellini, M. *Angew. Chem.* **1986**, *98*, 721. (l) Alexander, B. D.; Johnson, B. J.; Johnson, S. M.; Casalnuovo, A. L.; Pignolet, L. H. *J. Am. Chem. Soc.* **1986**, *108*, 4409 and references quoted therein.
(12) Gregory, B. J.; Ingold, C. K. *J. Chem. Soc. B* **1969**, 276.
(13) Mann, F. G.; Wells, A. F.; Purdie, D. *J. Chem. Soc.* **1937**, 1828.
(14) Sutton, B. M.; McGusty, E.; Walz, T.; Di Martino, M. J. *J. Med. Chem.* **1972**, *15*, 1095.
(15) Arnold, D. P.; Bennet, M. A. *Inorg. Chem.* **1984**, *23*, 2110.
(16) Fornies, J.; Green, M.; Spencer, J. L.; Stone, F. G. A. *J. Chem. Soc., Dalton Trans.* **1977**, 1006.
(17) Carmona, D.; Chaloupka, S.; Jans, J.; Thouvenot, R.; Venanzi, L. M. *J. Organomet. Chem.* **1984**, *275*, 303.
(18) McGilligan, B. S.; Venanzi, L. M.; Wolfer, M. *Organometallics*, in press.

**Table I.** Experimental Data[a] for the X-ray Diffraction Study of **2d**($CF_3SO_3$)

| | |
|---|---|
| formula | $C_{37}H_{46}AuF_8O_3PPt$ |
| mol wt | 1207.799 |
| cryst dimens, mm | 0.2 × 0.2 × 0.1 |
| cryst syst | monoclinic |
| space group | $P2_1/c$ |
| $a$, Å | 23.609 (5) |
| $b$, Å | 9.725 (4) |
| $c$, Å | 19.683 (5) |
| $\beta$, deg | 72.91 (2) |
| $Z$ | 4 |
| $V$, Å$^3$ | 4319.8 |
| $\rho$(calcd), g cm$^{-3}$ | 1.856 |
| $\mu$, cm$^{-1}$ | 68.56 |
| radiation | Mo K$\bar{\alpha}$ (graphite monochromated; $\lambda$ = 0.71069 Å) |
| measd reflcns | $\pm h,+k,+l$ |
| $\theta$ range, deg | $2.5 \le \theta \le 22.0$ |
| scan type | $\omega$ |
| max scan speed, deg min$^{-1}$ | 10.5 |
| scan width, deg | 1.20 + 0.35 tan $\theta$ |
| max counting time, s | 40 |
| prescan rejectn lim | 0.5 (2$\sigma$) |
| prescan acceptnce lim | 0.03 (33$\sigma$) |
| bkgd time | 0.5 × scan time |
| horiz receiving aperture, mm | 2.0 + tan $\theta$ |
| vert receiving aperture, mm | 4.0 |
| no. of indep data | 4756 |
| no. of obsd data [$F_o \ge 3\sigma(F_o)$] | 3862 |
| $R$[b] | 0.043 |
| $R_w$[c] | 0.050 |

[a] Collected at room temperature. [b] $R = \sum(|F_o| - |F_c|)/\sum|F_o|$. [c] $R_w = [\sum w(|F_o| - |F_c|)^2/\sum wF_o^2]^{1/2}$.

cell constants were determined on a Nonius CAD4/SDP diffractometer that was subsequently used for the data collection. The symmetry of the crystal is monoclinic, and from the systematic absences the space group was unambiguously determined as $P2_1/c$. Cell constants were obtained by a least-squares fit of 25 high-angle reflections ($10.0° \le \theta \le 15.9°$) using the CAD4 centering routines[19] and are listed along with crystallographic data and parameters for the data collection in Table I. Three reflections (10,0,$\bar{6}$; 543; 12,2,$\bar{2}$) were chosen as standards to check the stability of the crystal and of the experimental conditions and measured every 100 min; no significant variations were observed. The orientation of the crystal was checked by measuring three standard reflections (554; 10,0,8; 14,3,3) every 250. Data were collected at variable scan speed to ensure constant statistical precision of the measured intensities and were corrected for Lorentz and polarization factors; an empirical absorption correction was also applied to the data set by using azimuthal ($\psi$) scans of three reflections (1,3,$\bar{1}$; 2,4,$\bar{1}$; 2,6,$\bar{3}$) at high $\chi$ angle ($\chi \ge 85.5°$). Transmission factors were in the range 0.78–0.92. Data reduction and absorption correction were carried out by using the SDP[19] package. Reduced data were considered as observed if $F_o \ge 3.0\sigma(F_o)$, while an $F_o$ = 0.0 was given to the reflections having negative net intensities. The structure was solved by Patterson and Fourier methods and refined by block-diagonal least squares; the function minimized was $\sum w(|F_o| - (1/k)|F_c|)^2$ with weights chosen according to Cruickshank[20] and scattering factors taken from ref 21. The correction for the real part of the anomalous dispersion[21] was also taken into account. Anisotropic temperature factors were used for Au, Pt, P, and F atoms and for the $(CF_3SO_3)^-$ group, while isotropic factors were given to the remaining atoms. The contribution of the ligand H atoms in their idealized positions (C–H = 0.95 Å) was also taken into account but not refined. No extinction correction was applied. Upon convergence, a Fourier difference map revealed a strong peak between the metal atoms consistent with the presence of a bridging hydride. The peak persisted when a Fourier difference map was calculated with a limited data set[22] (cutoff limit (sin $\theta$)/$\lambda$ = 0.3 Å$^{-1}$), and therefore this H atom was included in the last cycles of refinement; its positional and thermal parameters converged satisfactorily even though with the expected high esd's. The final agreement factors are shown in Table I. A complete list of the final positional parameters is given in Table II.

**Table II.** Final Atomic Positional Parameters for **2d**($CF_3SO_3$)

| | $x/a$ | $y/b$ | $z/c$ |
|---|---|---|---|
| Pt | 0.17721 (2) | 0.17680 (6) | −0.01741 (3) |
| Au | 0.28332 (2) | 0.04553 (6) | −0.05375 (3) |
| $\mu$H | 0.22190 (397) | 0.07065 (917) | −0.08227 (470) |
| P1 | 0.37165 (16) | 0.01981 (40) | −0.03193 (21) |
| P2 | 0.21572 (20) | 0.36204 (44) | −0.09037 (24) |
| P3 | 0.13582 (18) | −0.01943 (40) | 0.04366 (24) |
| C1 | 0.11433 (62) | 0.30143 (145) | 0.04974 (73) |
| C2 | 0.06224 (74) | 0.32488 (170) | 0.03673 (88) |
| C3 | 0.01794 (78) | 0.40975 (183) | 0.08497 (92) |
| C4 | 0.02791 (79) | 0.46202 (183) | 0.13886 (95) |
| C5 | 0.07945 (81) | 0.44243 (180) | 0.15663 (97) |
| C6 | 0.12052 (75) | 0.35830 (177) | 0.11063 (91) |
| F1 | 0.04787 (37) | 0.27269 (102) | −0.01942 (52) |
| F2 | −0.03609 (42) | 0.43013 (112) | 0.06879 (72) |
| F3 | −0.01565 (59) | 0.54177 (123) | 0.18581 (72) |
| F4 | 0.09059 (62) | 0.49901 (135) | 0.21287 (60) |
| F5 | 0.17155 (45) | 0.33967 (116) | 0.12817 (52) |
| C1P1 | 0.43080 (59) | 0.08585 (138) | −0.10383 (70) |
| C2P1 | 0.43020 (74) | 0.04588 (169) | 0.17419 (88) |
| C3P1 | 0.47510 (82) | 0.09185 (199) | −0.23158 (99) |
| C4P1 | 0.52015 (81) | 0.16584 (188) | −0.22147 (97) |
| C5P1 | 0.52192 (84) | 0.21027 (198) | −0.15958 (100) |
| C6P1 | 0.47619 (76) | 0.16835 (170) | −0.09752 (90) |
| C7P1 | 0.39107 (55) | −0.15272 (127) | −0.01504 (67) |
| C8P1 | 0.43172 (72) | −0.22937 (176) | −0.06926 (89) |
| C9P1 | 0.44508 (83) | −0.36837 (198) | −0.05572 (101) |
| C10P1 | 0.41711 (75) | −0.42986 (174) | 0.00713 (89) |
| C11P1 | 0.37861 (73) | −0.35281 (171) | 0.06087 (88) |
| C12P1 | 0.36592 (68) | −0.21328 (158) | 0.04753 (81) |
| C13P1 | 0.37299 (62) | 0.11834 (146) | 0.04608 (73) |
| C14P1 | 0.41403 (70) | 0.09371 (168) | 0.08003 (84) |
| C15P1 | 0.41229 (74) | 0.16604 (169) | 0.14280 (88) |
| C16P1 | 0.37309 (74) | 0.27288 (184) | 0.16290 (90) |
| C17P1 | 0.33078 (73) | 0.29520 (171) | 0.12955 (87) |
| C18P1 | 0.32992 (67) | 0.21941 (161) | 0.06848 (80) |
| C1P2 | 0.21034 (93) | 0.53478 (212) | −0.04877 (109) |
| C2P2 | 0.25127 (111) | 0.54067 (251) | −0.00137 (134) |
| C3P2 | 0.28856 (141) | 0.34447 (323) | −0.15164 (168) |
| C4P2 | 0.33846 (184) | 0.40910 (446) | −0.14815 (220) |
| C5P2 | 0.16335 (114) | 0.40265 (274) | −0.14557 (138) |
| C6P2 | 0.15144 (102) | 0.28301 (247) | −0.18331 (122) |
| C1P3 | 0.18228 (79) | −0.10761 (190) | 0.09070 (94) |
| C2P3 | 0.19666 (92) | −0.01401 (218) | 0.14608 (111) |
| C3P3 | 0.06261 (76) | 0.00671 (183) | 0.10638 (92) |
| C4P3 | 0.03150 (96) | −0.13040 (228) | 0.14581 (115) |
| C5P3 | 0.12685 (79) | −0.14618 (184) | −0.01958 (94) |
| C6P3 | 0.08489 (94) | −0.09547 (226) | −0.06224 (112) |
| S | 0.70671 (27) | 0.32070 (62) | −0.27455 (29) |
| O1 | 0.72496 (72) | 0.30176 (128) | −0.34928 (63) |
| O2 | 0.67348 (106) | 0.43175 (261) | −0.25202 (110) |
| O3 | 0.68836 (91) | 0.19599 (222) | −0.23005 (99) |
| CF | 0.77251 (106) | 0.35510 (202) | −0.25694 (118) |
| F6 | 0.79585 (95) | 0.47603 (158) | −0.28535 (94) |
| F7 | 0.76392 (61) | 0.37578 (150) | −0.18642 (67) |
| F8 | 0.81182 (62) | 0.26444 (182) | −0.27690 (76) |

**Table III.** Selected Interatomic Distances (Å) and Bond Angles (deg) for Cation **2d**

| | | | |
|---|---|---|---|
| Au–Pt | 2.714 (1) | Pt–C1 | 2.07 (1) |
| Au–P1 | 2.264 (4) | Pt–$\mu$H | 1.74 (8) |
| Pt–P2 | 2.317 (4) | Au–$\mu$H | 1.72 (9) |
| Pt–P3 | 2.313 (4) | | |
| Pt–Au–P1 | 146.38 (3) | Pt–$\mu$H–Au | 103 (4) |
| Au–Pt–C1 | 151.51 (9) | P1–Au–$\mu$H | 172 (3) |
| Au–Pt–P2 | 92.2 (1) | C1–Pt–$\mu$H | 170 (4) |
| Au–Pt–P3 | 88.0 (1) | P2–Pt–$\mu$H | 88 (3) |
| P2–Pt–P3 | 173.0 (2) | P3–Pt–$\mu$H | 88 (3) |
| P2–Pt–C1 | 91.0 (4) | Au–Pt–$\mu$H | 38 (2) |
| P3–Pt–C1 | 92.1 (4) | Pt–Au–$\mu$H | 38 (2) |

## Results and Discussion

Silver(I) and gold(I) cations of the type $[M(solv)(PR''_3)]^+$ react with hydrido complexes of the type *trans*-$[PtH(R')(PR_3)_2]$ to give

(19) "Enraf-Nonius Structure Determination Package (SDP)"; Enraf-Nonius: Delft, Holland, 1980.
(20) Cruickshank, D. W. J. In *Computing Methods in Crystallography*; Ahmed, A., Ed.; Munksgaard: Copenhagen, 1972.
(21) *International Tables for X-Ray Crystallography*; Kynoch: Birmingham, England, 1974; Vol. IV.
(22) Teller, R. G.; Bau, R. *Struct. Bonding (Berlin)* **1981**, *44*, 1.

hydrido-bridged cations of the type $[(PR_3)_2(R')Pt(\mu\text{-}H)M(PR''_3)]^+$ (M = Ag (**1**), Au (**2**)). The cations prepared are as follows:

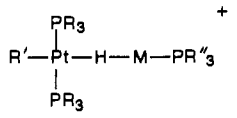

| | M | R | R′ | R″ |
|---|---|---|---|---|
| **1a** | Ag | Et | $C_6Cl_5$ | Et |
| **1b** | Ag | Et | $C_6Cl_5$ | *i*-Pr |
| **1c** | Ag | Et | $C_6Cl_5$ | Cy |
| **1d** | Ag | Et | $C_6Cl_5$ | Ph |
| **1e** | Ag | Me | $C_6Cl_5$ | *i*-Pr |
| **1f** | Ag | Me | $C_6Cl_5$ | Cy |
| **2a** | Au | Et | $C_6Cl_5$ | Et |
| **2b** | Au | Et | $C_6Cl_5$ | *i*-Pr |
| **2c** | Au | Et | $C_6Cl_5$ | Ph |
| **2d** | Au | Et | $C_6F_5$ | Ph |
| **2e** | Au | Et | Ph | Ph |
| **2f** | Au | *i*-Pr | Ph | Ph |

**Gold Complexes.** Complexes **2a–f** were obtained by adding solutions of complexes *trans*-$[PtH(R')(PR_3)_2]$, in THF, to solutions of the cations $[(Au(THF)PR''_3)]^+$ (prepared in situ by chloride abstraction with $Ag[BF_4]$ or $AgCF_3SO_3$ from the corresponding $[AuCl(PR''_3)]$ compound in THF), which had been precooled to −40 °C. The products isolated as $[BF_4]$ or $CF_3SO_3$ salts (with the exception of **2e**) are air-stable colorless solids. However, solutions of these complexes decompose fairly rapidly with deposition of metallic gold when allowed to warm to room temperature. The sequence of thermal stability of these solutions is

$$\mathbf{2b > 2a > 2c \simeq 2d > 2f > 2e}$$

Complex **2e** is so unstable that it could not be isolated, and its presence in solutions was demonstrated by its $^1H$ NMR spectrum.

It is noteworthy that the most stable complexes are obtained either when strongly electron-attracting aryl groups are bonded to platinum or when phosphines with electron-donor substituents on gold are employed. These observations and the formation of metallic gold mentioned earlier suggest that the mechanistic pathway for decomposition may consist of a hydride abstraction from platinum by the gold cation with transient formation of mononuclear $[AuH(PR_3)]$, which then, as expected, would decompose by an electron-transfer mechanism with formation of metallic gold. Obviously, the reaction

$$[(PR_3)_2(R')Pt(\mu\text{-}H)Au(PR''_3)]^+ + S \rightleftharpoons [(PR_3)_2(R')Pt(S)]^+ + [AuH(PR''_3)] \quad (1)$$

would be entropy-favored and, therefore, occur more easily at higher temperatures.

On the other hand, the presence of a strongly electron-attracting substituent on platinum would disfavor the above reaction, making the competitive process

$$[(PR_3)_2(R')Pt(\mu\text{-}H)Au(PR''_3)]^+ + S \rightleftharpoons [(PR_3)_2(R')PtH] + [(S)Au(PR''_3)]^+ \quad (2)$$

i.e., the reverse formation reaction, more favored.

Furthermore, the presence of a more basic phosphine on gold would also disfavor the hydride-abstraction reaction.

**X-ray Crystal Structure of $[(PEt_3)_2(C_6F_5)Pt(\mu\text{-}H)Au(PPh_3)](CF_3SO_3)$, 2d($CF_3SO_3$).** The solid-state structure of this compound consists of practically square-planar *trans*-$[PtH(C_6F_5)(PEt_3)_2]$ and almost linear "$AuH(PPh_3)$" units sharing the hydride ligand. A selection of bond lengths and angles is given in Table III, and ORTEP drawings of the cation and of the metal and donor atoms are shown in Figures 1 and 2. The hydride ligand could be localized, and the Pt–H–Au bond angle was found to be 103 (4)°, which can be taken as an indication that a strong, direct metal–metal interaction is occurring, consistent with the observed Pt–Au distance of 2.714 (1) Å. Comparable M–H–M′ bond angles have also been observed in the related species $[(CO)_5Cr(\mu\text{-}H)Au(PPh_3)]$ (Cr–H–Au = 111 (5)°[23] and

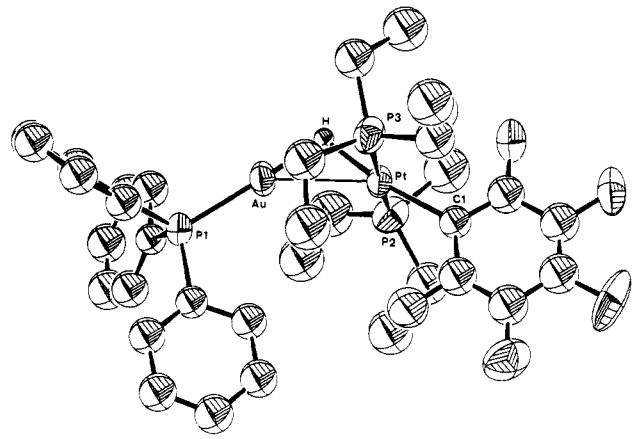


**Figure 1.** ORTEP drawing of the molecular structure of the $[(PEt_3)_2(C_6F_5)Pt(\mu\text{-}H)Au(PPh_3)]^+$ cation (**2d**).

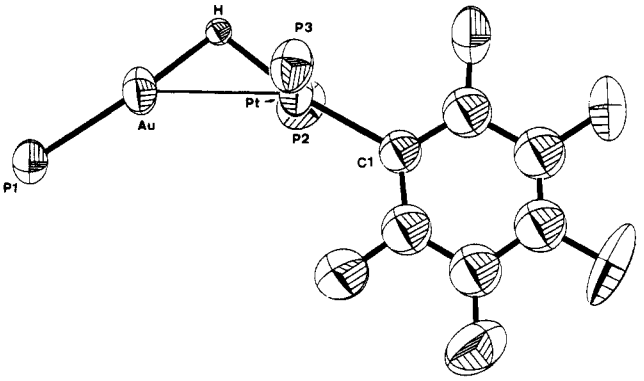


**Figure 2.** Relative positions of the metal and donor atoms in the cation $[(PEt_3)_2(C_6F_5)Pt(\mu\text{-}H)Au(PPh_3)]^+$ (**2d**).

$[(PPh_3)_3H_2Ir(\mu\text{-}H)Au(PPh_3)]^+$[8] (Ir–H–Au = 94°)[24] and $[(PEt_3)_2(C_6Cl_5)Pt(\mu\text{-}H)Ag(\mu\text{-}H)Pt(C_6Cl_5)(PEt_3)_2]^+$ (Pt–H–Ag = 109.0°).[25] These angles contrast with those found for symmetrical W–H–W[26] and Pt–H–Pt,[27] which fall in the range 123–160°. Thus the gold-containing compounds are likely to involve a stronger metal–metal interaction for which gold must be mainly responsible.

If one assumes (1) that this type of interaction is basically the same in all the gold complexes mentioned above and (2) that the gold cation $Au(PR''_3)^+$ is more likely to act as a net electron-acceptor than $Pt(R')(PR_3)_2^+$, one can discuss the interaction among Au, H, and M as follows: if one considers the isolobality of the gold cationic fragment with a proton and the Pt–H fragment as isolobal with $H_2$, one could imagine the interaction as analogous to that leading to $H_3^+$ from $H^+$ and $H_2$.[28] The extent of the direct M–M′ interaction in a bimetallic system of the type $L_nM(\mu\text{-}H)M'L'_m$ can be qualitatively related to the electron-donor capacity of the neutral $MHL_n$ fragment and the electron-acceptor capacity of the coordinatively unsaturated $M'L'_m$ cationic species. As the gold $Au(PR_3)$ cation is more strongly coordinatively unsaturated than the $Pt(C_6X_5)(PR_3)_2$ cation, at parity of electron donor, e.g., $[PtH(C_6X_5)(PEt_3)_2]$, one can expect a stronger Au–Pt interaction in the former case. Indeed, the Pt–Au distance in the Au–Pt compound is 2.714 (1) Å, while it is 3.011 (2) Å in $[(PMe_3)_2(C_6F_5)Pt(\mu\text{-}H)Pt(C_6F_5)(PMe_3)_2]^+$.[25] Similar consid-

(23) Green, M.; Orpen, A. G.; Salter, I. D.; Stone, F. G. A. *J. Chem. Soc., Dalton Trans.* **1984**, 2497.
(24) Calculated from the data of ref 8 by using the program HYDEX (see: Orpen, A. G. *J. Chem. Soc., Dalton Trans.* **1980**, 2509).
(25) Wolfer, M. Dissertation No. 8151, ETH Zürich, 1986.
(26) Love, R. A.; Chin, H. B.; Koetzle, T. F.; Kirtley, S. W.; Whittlesey, B. R.; Bau, R. *J. Am. Chem. Soc.* **1976**, *99*, 4491 and references quoted therein.
(27) Carmona, D.; Thouvenot, R.; Venanzi, L. M.; Bachechi, F.; Zambonelli, L. *J. Organomet. Chem.* **1983**, *250*, 589 and references quoted therein.
(28) Gimarc, B. M. *Molecular Structure and Bonding: The Qualitative Molecular Orbital Approach*; Academic: New York, 1979; p 23.

**Table IV.** NMR Data for Cations $[(PR_3)_2(R')Pt(\mu\text{-}H)M(PR''_3)]^+$ [a]

| | $^1$H NMR | | | | | $^{31}$P NMR | | | | |
|---|---|---|---|---|---|---|---|---|---|---|
| complex | $\delta$(Pt,H,M) | $^1J$(Pt,H) | $^1J$(Ag,H)[b] | $^2J$(P$^1$,H) | $^2J$(P$^2$,H) | $\delta$(P$^1$,P$^2$) | $^1J$(Pt,P$^2$) | $^1J$(Ag,P$^1$)[b] | $^3J$(Pt,P$^1$) | $T$, K |
| **1a** | −7.97 | 590 | 97 | *c* | *c* | 12.4/12.4 | 2297 | 567/653 | 212 | 203 |
| **1b**[d] | −8.10 | 594 | 90/104 | 35 | 14 | 50.3/10.5 | 2310 | 553/638 | 194 | 213 |
| **1c**[e] | −8.00 | 606 | 81/93 | 34 | 15 | 41.8/9.0 | 2315 | 566/652 | 161 | 183 |
| **1d** | −7.82 | 610 | 93 | 34 | 15 | 13.6/10.7 | 2319 | 550/636 | 187 | 203 |
| **1e**[f] | −7.51 | 629 | 79/91 | 34 | 15 | 49.1/−20.5 | 2258 | 570/659 | 168 | 178 |
| **1f** | −7.67 | 628 | 90 | *c* | 15 | 45.0/−20.7 | 2245 | 557/644 | 190 | 183 |
| **2a** | −4.73 | 537 | | 78 | 11 | 43.7/13.7 | 2321 | | 274 | 298 |
| **2b**[g] | −4.54 | 536 | | 74 | 10 | 71.3/10.8 | 2307 | | 257 | 298 |
| **2c** | −4.77 | 527 | | 84 | 10 | 40.6/11.5 | 2306 | | 278 | 298 |
| **2d** | −3.89 | 559 | | 82 | 10 | 40.0/17.9 | 2179 | | 328 | 298 |
| **2e** | −2.68 | 466 | | 96 | 9 | *h* | *h* | | *h* | 298 |
| **2f** | −3.69 | 437 | | 94 | 10 | 39.3/38.6 | 2529 | | 201 | 298 |

[a] Measured in $CD_2Cl_2$, at temperatures between −70 and −90 °C, except where otherwise indicated. Coupling constants ($J$) are given in Hz. [b] The two values refer to coupling to $^{107}$Ag (51.8%) and $^{109}$Ag (48.2%), respectively. Only one value is given; this corresponds to the average arising from the unresolved $^1J(^{107}Ag,^1H)$ and $^1J(^{109}Ag,^1H)$ values. [c] Not resolved. [d] $^3J(Ag,P^2) = 4$; $\delta(Pt) = -4807$, $^2J(Pt,Ag) = 409$. [e] In $CD_3COCD_3$; $^3J(Ag,P^2) = 4$; $\delta(Pt) = -4803$, $^2J(Pt,Ag) = 420$. [f] In $CD_3COCD_3$; $^3J(Ag,P^2) = 4$; $\delta(Pt) = -4775$, $^2J(Pt,Ag) = 440$. [g] $^4J(P^1,P^2) = 2$. [h] Not measured.

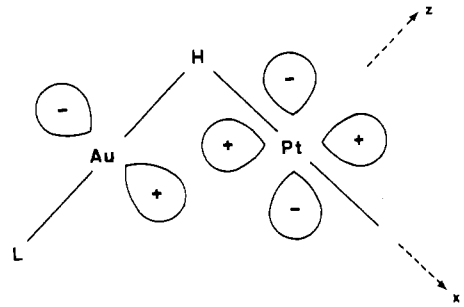


**Figure 3.** Qualitative orbital diagram for the direct metal–metal interaction in cations of the type $[(PR_3)_2(C_6X_5)Pt(\mu\text{-}H)M(PR'_3)]^+$ (X = F, Cl; M = Ag, Au).

erations apply also to the Au–Ir and Au–Cr complexes mentioned earlier.

A possible qualitative orbital interaction scheme for the Pt–Au complex is shown in Figure 3.

**Silver Complexes.** Complexes **1a–f** were prepared by adding 1 equiv of the corresponding platinum hydride species to solutions containing 1 equiv of $Ag[BF_4]$ or $AgCF_3SO_3$ and 1 equiv of the corresponding phosphine $PR''_3$. The salts with the above anions can be obtained in crystalline form when *trans*-$[PtH(C_6Cl_5)(PEt_3)_2]$ is used as a "hydride-donor", while the corresponding species where $PMe_3$ is used instead of $PEt_3$, i.e., complexes **1e** and **1f**, can be obtained only as amorphous powders. Both sets of solids are, however, colorless and air-stable although slightly photosensitive.

As found for the related compounds $[(PR_3)_2(C_6Cl_5)Pt(\mu\text{-}H)HgR]^+$,[18] the complexes that contain $PMe_3$ bonded to platinum are less thermally stable than the corresponding compounds containing $PEt_3$. Although is cannot be excluded that this effect could be due to electronic factors, it appears likely that it is mainly of steric origin. Thus, the use of $PEt_3$ as coligand in complexes of the type *trans*-$[PtH(C_6X_5)(PR_3)_2]$ (X = F, Cl) prevents the formation of the hydrido-bridged complexes $[(PEt_3)_2(C_6X_5)Pt(\mu\text{-}H)Pt(C_6X_5)(PEt_3)_2]^+$, while the corresponding species with $PMe_3$ can be easily obtained.[25] This difference is likely to be due to steric effects: one would expect a compensation of the electronic factors, as the higher (or lower) electron-donor capacity of, e.g., *trans*-$[PtH(C_6Cl_5)(PMe_3)_2]$, relative to that of its $PEt_3$ analogue, would be compensated by the expected lower (or higher) electron-acceptor capacity of the *trans*-$Pt(C_6Cl_5)(PMe_3)$ fragment. As differences of steric effect between $PMe_3$ and $PEt_3$ appear to hinder hydrido-bridge formation, it is possible that the formation of the Pt–H–Ag bridge is more favored when $PMe_3$ is coordinated to platinum.

Furthermore, if it is assumed that the molecular geometry of the Pt–H–Ag bridge is similar to that found for the Pt–H–Au bridge, one could expect a stronger Pt–Ag coupling (both indirect through the hydride ligand and direct through the metal–metal bonding). The lower stability of the complexes with trimethylphosphine would then be due to a greater electron-withdrawing capacity of the more strongly bonded silver atom eventually resulting in permanent electron transfer.

In general, thermal stabilities of the silver-containing complexes are higher than those of the corresponding gold complexes. This observation may be attributed to the higher electron affinity of gold relative to silver cations and the consequent electron-transfer process mentioned earlier.

Although up to now it has not proved possible to obtain single crystals of suitable size for X-ray diffraction of complexes of type **1**, available structural and NMR data (see later) indicate that corresponding gold and silver complexes should not show major structural differences either in solution or in the solid state.

However, NMR measurements (see later) show that when compounds of type **1** are dissolved in solvents such as acetone or dichloromethane, the following disproportionation reaction for compound **1c** occurs:

$$2[\mathbf{1c}] \rightleftharpoons \underset{\mathbf{3a}}{[(PEt_3)_2(C_6Cl_5)Pt(\mu\text{-}H)Ag(\mu\text{-}H)Pt(C_6Cl_5)(PEt_3)_2]^+} + \underset{\mathbf{4c}}{[Ag(PCy_3)_2]^+} \quad (3)$$

The equilibrium constant $K_{disp}$ for this process in $CH_2Cl_2$ at −60 °C is ca. $10^{-2}$. It should be noted that a mixture of **1c**, **3a**, and **4c** in the above proportions is obtained on mixing equimolecular amounts of **3a** and **4c**. NMR measurements indicate that the other complexes **1a,b** and **1d–f** show similar behavior and that the values of $K_{disp}$ do not significantly change with changes of phosphine.

The full characterization of cations **3**, including neutron diffraction data on a related complex, will be described in a subsquent publication.[29]

**NMR Spectroscopy.** Multinuclear NMR studies were conducted on complexes of types **1** and **2**. The data are summarized in Table IV.

Although the gold-containing complexes are less thermally stable, they are less dynamic in solution than the corresponding silver complexes. Thus, while complexes of type **2** give sharp signals at room temperature, in order to obtain spectra corresponding to static structures for complexes of type **1**, temperatures below −40 °C are required.

The NMR spectra of the gold complexes show that the solid-state structure is retained in solution. Thus, the $^{31}P\{^1H\}$ spectra show two sets of signals, the pseudotriplet arising from the phosphorus atoms bonded to platinum, $P^2$, with the corresponding satellites and a signal due to the phosphorus bonded to gold, $P^1$, which also shows platinum satellites with a $J$(P,Pt) in the range 200–300 Hz. In the case of compound **2b**, even a small (2-Hz) $P^1,P^2$ coupling is observed, resulting in the main signal due to $P^1$

(29) Albinati, A.; Koetzle, T. F.; Venanzi, L. M.; Wolfer, M., to be submitted for publication.

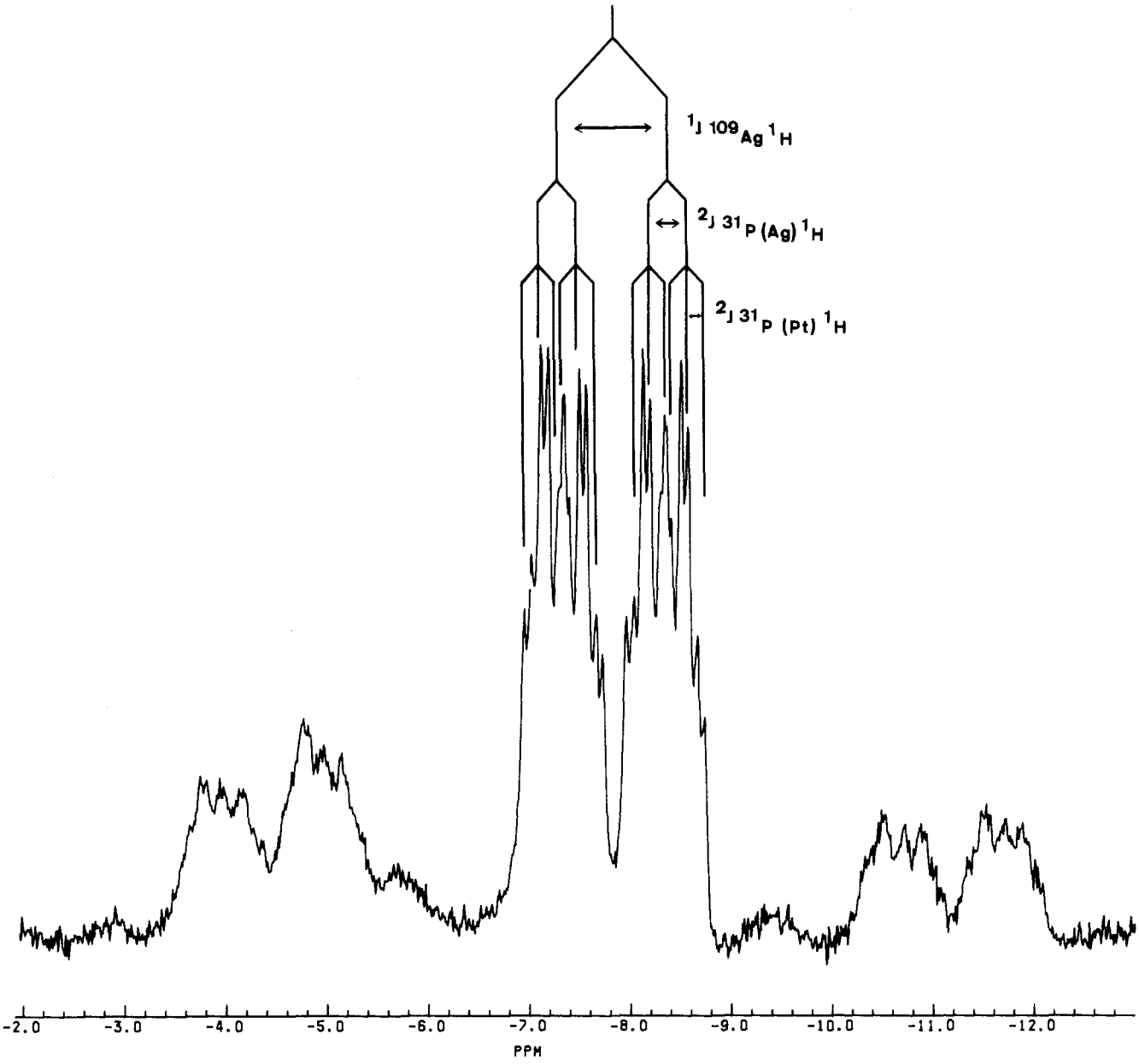


**Figure 4.** Hydride region of the $^1$H NMR spectrum of $[(PEt_3)_2(C_6Cl_5)Pt(\mu\text{-}H)Ag(PPh_3)]^+$ (**1d**) at 250 MHz and 183 K in $CD_3COCD_3$.

appearing as a triplet and that due to $P^2$ appearing as a doublet. The $^1$H spectrum in the hydride region shows the expected doublet of triplets flanked by the corresponding $^{195}$Pt satellites.

As mentioned earlier, the NMR spectra of solutions of complexes **1a–f** show that equilibria of type **3** are present in solution, although complexes of type **1** are the predominant species observed when the Pt:Ag:$P^1R_3$ ratio is 1:1:1. The spectral data for complexes of type **3** and the X-ray crystal structure of compound **3a** have been described elsewhere[25] and will be published in a subsequent paper.[29] The $^{31}P\{^1H\}$ NMR spectra of compounds of types **1a–f** are of the same basic type as those of the corresponding gold complexes with the exception of the presence of couplings due to the $^{107}$Ag and $^{109}$Ag isotopes (natural abundance 51.82 and 48.18%, respectively). While the $^1J(Ag,P^1)$ coupling is large (e.g., 550–570 Hz for $^{107}$Ag), that with $P^2$ is small (e.g., ca. 4 Hz), and thus it has not been possible to observe it for all the complexes. The formation of a Pt–H–M (M = Ag, Au) bridge is supported also by the observation of a $J(Pt,P^1)$ coupling[30] that is of the order 160–210 Hz for M = Ag and 200–330 Hz for M = Au. The $^1$H NMR spectra, in the hydride region, are much more complex than those of the corresponding gold compounds because of the additional $^{107}$Ag and $^{109}$Ag couplings. The signals due to the hydride ligand in compound **1d** are shown in Figure 4. The main set of signals can be analyzed on the basis of a first-order spectrum, and the relevant parameters are shown in Table IV. As expected, the $^{195}$Pt satellites are broad because of relaxation due to "chemical shift anisotropy".[31]

As found for other hydrido-bridged platinum complexes, e.g., $[(PR_3)_2(R')Pt(\mu\text{-}H)Pt(R'')(PR_3)_2]^+$ (R′ or R″ = H or aryl),[27] the $^1J(Pt,H)$ coupling constant of the hydride ligand in the parent mononuclear complex, e.g., *trans*-[PtH(R′ or R″)$(PR_3)_2$], decreases on the hydrido-bridge formation. The $\Delta J(Pt,H)$ values for the gold complexes are slightly larger than those for the corresponding silver complexes ($\Delta J(Au) \simeq 190$ Hz and $\Delta J(Ag) \simeq 140$ Hz). The corresponding change in the diplatinum complexes mentioned earlier is of 327 Hz for the pair *trans*-[PtH$(C_6Cl_5)(PMe_3)_2$] and $[(PMe_3)_2(C_6Cl_5)Pt(\mu\text{-}H)Pt(C_6Cl_5)(PMe_3)_2]^+$.[25] The hydride chemical shifts in the Pt/Au and Pt/Ag

(30) The values of these constants are to be considered as the combination of two contributions, one formally written as $^2J(^{195}Pt,^{31}P)$, which goes through the direct Pt–Ag metal bond, and the other given by $^3J(^{195}Pt,^{31}P)$, i.e., the coupling occurring through the Pt–H–Ag moiety.

(31) Lallemand, J. Y.; Soulié, J.; Chottard, J. C. *J. Chem. Soc., Chem. Commun.* **1980**, 436.

Table V. $^{31}P\{^1H\}$ NMR Parameters for Cations $[Ag(PR_3)_2]^+$ (4) (Measured in $CD_3COCD_3$ at −80 °C)

| complex | $\delta(^{31}P)$ | $^1J(^{107}Ag,^{31}P^1)$, Hz | $^1J(^{109}Ag,^{31}P)$, Hz |
|---|---|---|---|
| **4a** | 8.3 | 484 | 558 |
| **4b** | 43.9 | 468 | 540 |
| **4c** | 40.3 | 446 | 515 |
| **4d** | 10.7 | 492 | 530 |

compounds occur at lower fields than in the corresponding mononuclear platinum complexes. These low-field shifts are larger for the gold compounds (ca. 5 ppm) than for the silver complexes (ca. 2 ppm). It is noteworthy that these low-field shifts on bridge formation appear to be qualitatively related to the thermal stability of the bimetallic compounds, as the $\Delta\delta$ values of the related Pt/Hg complexes of the type $[(PEt_3)(C_6Cl_5)Pt(\mu\text{-}H)HgR]^+$, which decompose above −40 °C, are of the order of ca. 8 ppm.[18]

Corresponding changes are also observed in parameters such as $^1J(Pt,P^2)$ and $^2J(P,H)$ (see Table IV). While in the former case the changes of these parameters on bridge formation are more comparable in the gold and silver compounds ($\Delta J \simeq 450$ Hz), in the latter case the $\Delta J(Au)$ values are ca. 8 Hz and $\Delta J(Ag)$ values are ca. 3 Hz.

All the above data can be taken as an indication that the Au–H bond is likely to be stronger than the corresponding Ag–H bond.

In this context it is noteworthy that when complexes such as *trans*-$[PtH(C_6Cl_5)(PEt_3)_2]$ are reacted with species such as $Cu(P\text{-}i\text{-}Pr_3)^+$ cations, no interaction can be detected even at ca. −70 °C.

Finally, the values of the Pt,Ag-coupling constants in complexes **1b**, **1c**, and **1e** are of the order of 400 Hz. The relationship between these values and the degree of Pt–Ag interaction is unclear, particularly because very few Pt–Ag constants are known, e.g., those published by van der Ploeg et al.,[32] which, however, are for compounds of very different structures. Thus the $J(Pt,Ag)$ values in compounds of type **5** are of the order of ca. 170 Hz.

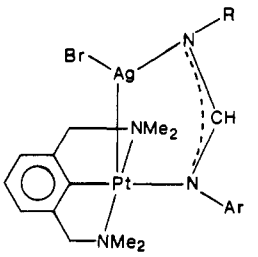


**5**

However, as can be seen from their structure, the Pt–Ag interactions are very different from those occurring in complexes containing Pt–H–Ag bridges.

As solutions of compounds of type **1** also contain the cations $[Ag(PR_3)_2]^+$ (**4**), their $^{31}P$ NMR parameters are listed in Table V. The values of the $^1J(Ag,P)$ coupling constants are of the order of magnitude expected for two-coordinate silver.[33]

**Acknowledgment.** H.L. and M.W. received support from the Swiss National Science Foundation, and A.A. acknowledges financial support from the Italian MPI. We are greatly indebted to Dr. P. S. Pregosin for valuable discussion and S. Chaloupka for experimental assistance.

**Supplementary Material Available:** Figure S1, showing the numbering scheme, and Tables S1 and S2, giving final positional and thermal parameters and an extended list of bond lengths and angles (5 pages); Table S3, listing observed and calculated structure factors (16 pages). Ordering information is given on any current masthead page.

(32) Van der Ploeg, D. F. M. J.; van Koten, G.; Brevard, C. *Inorg. Chem.* **1982**, *21*, 2878.

(33) Camalli, M.; Caruso, F.; Chaloupka, S.; Kapoor, P. N.; Pregosin, P. S.; Venanzi, L. M. *Helv. Chim. Acta* **1984**, *67*, 1603 and references quoted therein.

Contribution from the Departments of Chemistry and Physics, Syracuse University, Syracuse, New York 13244-1200

# Gas-Phase One-Photon Electronic Spectroscopy of (Arene)chromium Tricarbonyls: Substituent Effects in Multiphoton Dissociation/Ionization Spectra

Dan Rooney,† J. Chaiken,*† and D. Driscoll‡

*Received January 15, 1987*

We have measured the first gas-phase electronic absorption spectra of $(\eta^6\text{-}C_6H_6)Cr(CO)_3$, $(\eta^6\text{-}C_6H_5Cl)Cr(CO)_3$, and $(\eta^6\text{-}C_6H_5CH_3)Cr(CO)_3$. Low-resolution, 200-$cm^{-1}$, spectra show intense (92 000 L/(mol cm)) absorption features extending into the vacuum ultraviolet region indicating the existence of at least five different electronic states with energies below 61 000 $cm^{-1}$. Our low-resolution data suggest that only one of those states shifts appreciably with arene substitution. We compare these results with solution-phase spectra and other data. At higher resolution, 40 $cm^{-1}$, our data suggest that the onset of detectable absorption is lower in energy for $(\eta^6\text{-}C_6H_6)Cr(CO)_3$ than for both $(\eta^6\text{-}C_6H_5Cl)Cr(CO)_3$ and $(\eta^6\text{-}C_6H_5CH_3)Cr(CO)_3$. The fine structure of this transition may be correlated with the well-known photolability of the CO ligands. We discuss these new data in the light of our earlier multiphoton spectroscopy results on these molecules.

## Introduction

There are relatively few gas-phase one-photon UV–visible absorption spectra available for organometallic molecules, especially those with non-carbonyl ligands, yet such spectra provide valuable information concerning electronic structure and bonding. The nature of the $\eta^6$ Cr–arene bond in $(\eta^6\text{-arene})Cr(CO)_3$ complexes and the effects of coordination on the electronic structure[1-3] and reactivity patterns[4,5] of the arene ligand are questions of

† Department of Chemistry.
‡ Department of Physics.

(1) Eisenstein, O.; Hoffmann, R. *J. Am. Chem. Soc.* **1981**, *103*, 4308 and references therein.
(2) Elian, M.; Chen, M. M. L.; Mingos, D. M. P.; Hoffmann, R. *Inorg. Chem.* **1976**, *15*, 1148.
(3) Albright, T. A.; Hofmann, P.; Hoffmann, R. *J. Am. Chem. Soc.* **1977**, *99*, 7546.

0020-1669/87/1326-3939$01.50/0 